Current Science
CS 5 (3), 2180-2198 (2025)
Received 16 Feb 2025 | **Revised 15 March** 2025 | **Accepted 13 April**. 2025 | **Online Available 6 May** 2025
https://doi.org/ 10.52845/CS/2025-5-3-12

Current Science

Current Science

OPEN ACCESS

ISSN(O)2795-8639

Orignal Article

Rebar Price Prediction using Stacking Methods: A Comparative Analysis of LSTM and Neuralprophet Fusion Models

Jingsi Hao[1], Xiakai Wang[2], Zhonghua Yang[1], Yuanyuan Zhao[1], Kangjie Sun[1]*

[1]Hebei University of Science and Technology 050018, China

[2]Huawei HiSilicon 518100, China

***Corresponding Author: Kangjie Sun**

Abstract:
The fluctuation in rebar prices directly impacts the production costs in industries such as construction and metallurgy. Accurate price prediction is crucial for informed decision-making in these sectors. Traditional time series forecasting methods, however, are insufficient in capturing the nonlinear characteristics of price fluctuations, In recent years, deep learning-based methods, such as NP(NeuralProphet) and LSTM(Long Short-Term Memory Networks), have become popular in time series forecasting due to their strong sequence modeling capabilities. This paper proposes a stacking method to create a hybrid NP-LSTM forecasting model, combining NP and LSTM models to enhance the accuracy of rebar price predictions on a monthly basis. Compared to the individual NP and LSTM models, the NP-LSTM hybrid model combines the strengths of both, compensating for their weaknesses and providing more accurate predictions. This approach enhances both model performance and its stability and reliability in real-world applications, offering significant practical value. This study demonstrates the effectiveness of the stacking method for multi-model fusion, offering a novel approach to rebar price prediction.

Keywords Price expectation, Multi-variable, NeuralProphet model, Long Short-Term Memory Networks optimization model, Stacking technique.

Introduction

The sustained and rapid growth of China's economy has led to a corresponding increase in large-scale infrastructure construction and real estate development, driven by the demand for urbanization[1,2].Rebar, one of the most commonly used steel construction materials, is essential in various construction projects, including residential housing, corporate plants, transportation infrastructure, and public welfare projects such as dams, high-speed rail bridges, highways, and municipal roads [3-5].Between 2010 and 2021, China's annual steel production increased from over 600 million tons to more than 1 billion tons. In 2021, China's annual steel consumption reached nearly 1 billion tons, with the output value of the iron and steel industry contributing about 4.5% to the country's GDP, highlighting its significant economic impact. Moreover, the high consumption coupled with rebar's unique financial characteristics (He et al., 2017) has made it indispensable in the production of steel end products[6-13].Consequently, accurate and timely forecasting of rebar prices is of significant practical importance. However, rebar prices are highly sensitive to volatile factors such as macroeconomic conditions, policy shifts, and financial activities [14-18]. As a result, traditional forecasting methods often fail to reflect market changes accurately and promptly, making it difficult to meet the industry's increasing demand for higher forecasting accuracy and efficiency.

Given the significance of rebar price trends, an increasing number of scholars are focusing on rebar price prediction methods [19-25].However, accurately predicting rebar prices in a timely manner remains challenging, and no prediction method can consistently provide accurate results.

The difficulty in predicting material prices can be attributed to the limitations of forecasting methods. Rebar price prediction methods can generally be divided into two categories: the factor prediction method, which establishes the relationship between various factors and the predicted value 26.Due to its inherent rationality and causality, many scholars employ the factor prediction method for rebar price forecasting. For instance, the ARIMA model, widely studied by some scholars, uses the predictive information of different lags of the target variables [27,28].Other scholars use the VAR model, which incorporates the economic relationships between different variables, thereby expanding the predictive information compared to the ARIMA model [29,30].While factor forecasting is rational and accurate, the challenges of factor selection and determination have led many scholars to turn to time series methods for forecasting industrial metal prices.

Time series forecasting methods can be broadly classified into two categories: monolithic models and hybrid models. Monolithic forecasting methods primarily focus on neural network algorithms, classical forecasting techniques, and particularly deep learning methods. For instance, Zhao et al. employed an LSTM neural network to construct an oil exchange rate risk warning model, significantly improving prediction accuracy and risk warning performance 31.Wang et al. developed a BP neural network model that performs well in 30-day coal price prediction, with higher accuracy than LSTM and ARIMA models 32.Although single models perform well in certain areas, they still have limitations in accuracy and applicability. As a result, hybrid prediction models have gained attention as a research focus in recent years. Hybrid models effectively compensate for the limitations of single models by combining the strengths of multiple forecasting methods. Yadav A K and Vishwakarma V P combined LSTM with convolutional layers to predict stock prices, achieving better prediction accuracy than the baseline model 33.Jana R K et al. developed a Prophet-LSTM-BP hybrid model to forecast electricity load values 34.Additionally, Hu et al. (2020) developed an integrated model for copper price prediction, combining ANN-LSTM and the GARCH statistical model, and verified its effectiveness through experiments 35.

A review of previous work reveals that deep learning-based time series prediction methods are becoming mainstream, with LSTM (Long Short-Term Memory Network) being one of the most widely used models due to its superior ability to capture time-dependent patterns. NeuralProphet, an extension of the traditional Prophet model, effectively models seasonality, holiday effects, exogenous variables, and other factors. Few scholars have explored combining factor forecasting with time series forecasting. To address these limitations, a novel forecasting architecture is proposed, integrating the NeuralProphet and LSTM models through the stacking method [36-38]to predict rebar prices.

Based on the previous research, the main contributions of this paper are as follows:

1. A novel method for constructing a forecasting model based on both factor and time series forecasting is proposed. This method is applied to rebar monthly price prediction. Traditional forecasting methods mainly involve factor forecasting, which considers the relationships between various variables, or time series forecasting alone 39.This paper considers both time and influencing factors to gather more information, constructing a single model to forecast rebar price trends over a long period (20 months).This allows for a better understanding of long-term rebar price trends.
2. This study analyzes and selects relevant factors affecting rebar prices using three methods: gray correlation analysis (GRA), multilayer feed-forward neural networks (MLP), and Pearson correlation coefficient analysis.
3. This paper uses the stacking method to enhance rebar price prediction accuracy by combining monolithic models into a hybrid prediction model. Studies have shown that the hybrid prediction model achieves higher accuracy than the monolithic model [40-42].Therefore, it can be concluded that the hybrid prediction model effectively compensates for the deficiencies of the monolithic model.
4. Time factors and other influencing variables are used to construct NP, optimized LSTM, and BP neural network monolithic models to

predict rebar prices over 20 periods (20 months). The NP-LSTM, NP-BP, and LSTM-BP hybrid prediction models are constructed by stacking the monolithic prediction models.

2 Methodology

2.1 Constructing a monolithic model

2.1.1 Modeling the NP Monomer

NeuralProphet is a powerful tool that combines the strengths of deep learning with traditional time series modeling, making it particularly effective in capturing complex seasonal and nonlinear trends. In many real-world applications, NeuralProphet has outperformed traditional time series models, particularly when data exhibit complex cyclical variations and nonlinear trends. With its neural network-based seasonality and trend modeling capabilities, NeuralProphet offers significant advantages in long-term time series forecasting, particularly for data with seasonal fluctuations and external events such as holidays. Consequently, this model is ideal for datasets with complex time-dependent structures.

The core concepts of NeuralProphet align with those of Prophet, both featuring modularity and composability, enabling users to flexibly select and combine model components based on their needs. Each component adds functionality for time series prediction, thereby enhancing the model's flexibility and scalability. The model first captures the long-term trend of the time series to identify trend changes, then accounts for cyclical fluctuations (e.g., annual and weekly cycles) to accurately capture seasonal patterns. Additionally, NeuralProphet adjusts for the impact of external events, such as holidays and promotions, to improve forecasting accuracy. To better capture short-term dependencies, NeuralProphet includes an autoregressive component, essential for forecasting rapid fluctuations. The model also incorporates external features (exogenous variables) to enhance forecasting capabilities and captures unexplained noise through residual terms to improve accuracy. Most components can be scaled by trend for a multiplicative effect, or the time series can be decomposed into multiple components, allowing NeuralProphet to better capture complex patterns in the data. The mathematical expression is (1):

$$\hat{y}_t = T(t) + S(t) + H(t) + A(t) + F(t) + \in_t \quad (1)$$

Formula $T(t)$——	Trend component, representing long-term trend changes in the time series
$S(t)$——	Seasonal component, capturing cyclical fluctuations in the time series (e.g., annual and weekly cycles)
$H(t)$——	Represents the impact of special events or holidays at time t
$A(t)$——	Autoregressive component for modeling short-term historical dependencies
$F(t)$——	Impact of future known external features (exogenous variables)
$\in_t$——	Residual terms, representing unexplained noise

Using (1) , the NeuralProphet model combines multiple components to construct a robust time series forecasting model. The following outlines the construction process of the NeuralProphet model:

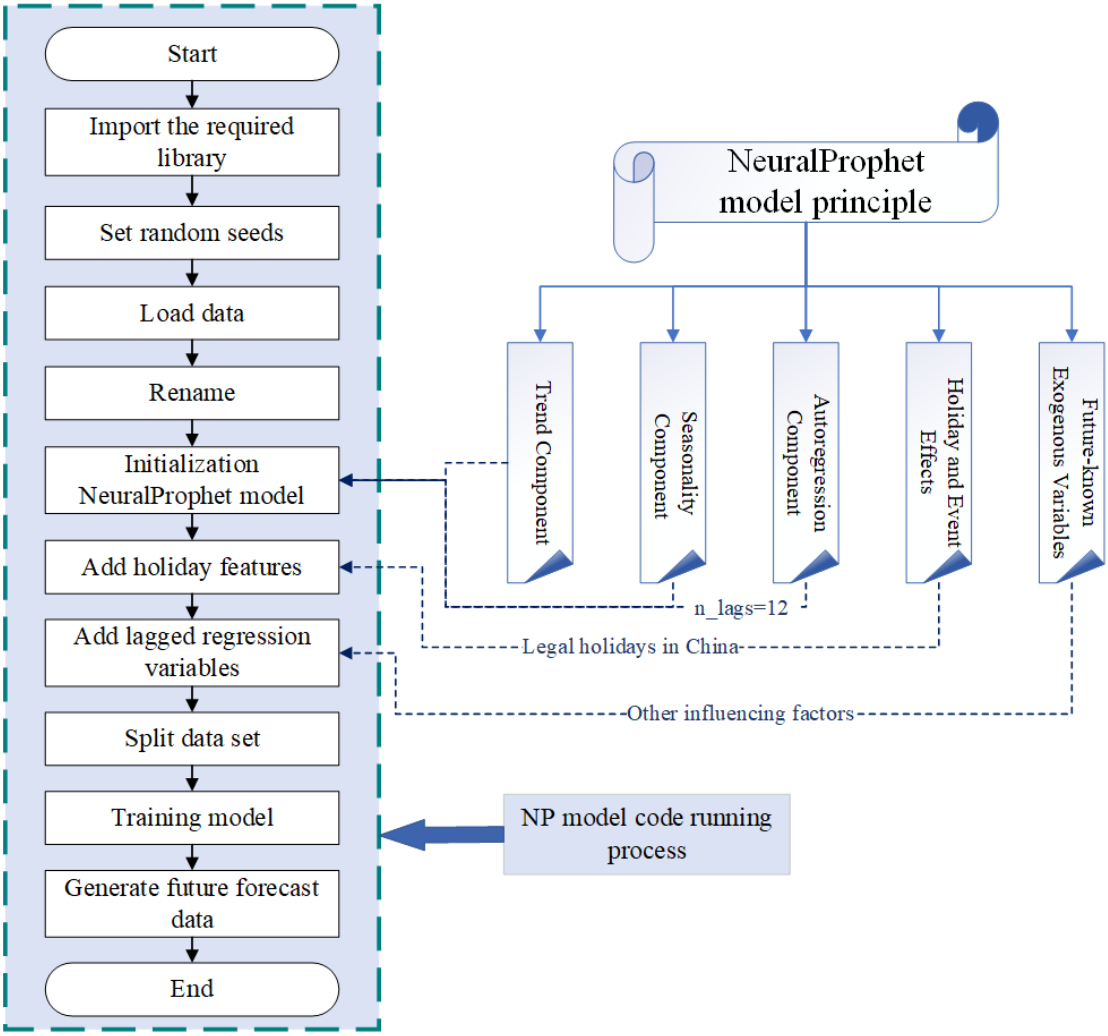

Figure 1 NeuralProphet prediction model process

Figure 1 illustrates the NeuralProphet model construction and prediction process, which consists of the following steps: data preparation and preprocessing to ensure proper content and format; model selection and configuration to initialize the NP model, select appropriate components (e.g., trends, seasonality, holiday effects, external features), and adjust their parameters based on data characteristics; model training, where historical data is used to train the NP model, allowing it to learn trends, seasonality, and other influences by minimizing prediction error through an optimization algorithm (e.g., Adam).During training, the neural network adjusts internal parameters to minimize prediction error. The prediction results are saved, and after training is complete, the NP model can be used to make predictions for future time points. The prediction results are combined with trend, seasonality, holiday effects, historical dependencies, and external features to generate a comprehensive forecast, which is then saved.

NeuralProphet integrates traditional time series models with modern deep learning techniques to capture complex seasonality, non-linear trends, and the effects of external events in time series data. Its modular design provides high flexibility and scalability, enabling users to adjust and optimize it for various application scenarios. By incorporating trend modeling, seasonality modeling, holiday effects, and other components, NeuralProphet captures complex patterns in time series, resulting in higher forecasting accuracy compared to traditional methods in real-world applications.

2.1.2 Constructing LSTM Monolithic Models

LSTM (Long Short-Term Memory) is a specialized type of recurrent neural network (RNN) designed to address the long-term dependency problem by enhancing the memory units of traditional RNNs. The key innovation of LSTM lies in its internal structure of multiple "gates" that determine what information to retain

and what to discard, providing a significant advantage when processing long data sequences.

The core component of the LSTM is the Cell State, which stores long-term memories for the network. LSTM controls the flow of information through three gates: the forget gate, input gate, and output gate. Each gate has a specific function and regulates the storage and output of information via control signals.

The main computation in LSTM is performed through the combination of these three gates and memory cells.

The Forget Gate determines how much of the past memory is discarded at each time step. Its output is a value between 0 and 1, where 0 means complete forgetting and 1 means complete retention. The formula is calculated using a Sigmoid activation function, represented by the following mathematical expression (2):

$$f_t = \sigma(W_f \cdot [h_{t-1}, x_t] + b_f) \quad (2)$$

Formula

f_t—— Output of the Oblivion Gate

h_{t-1}—— Hidden state from the previous moment

x_t—— Input features at the current time

W_t—— Weighting of the Oblivion Gate

b_f—— Bias of the Oblivion Gate

The Input Gate controls how the current input influences the state of the memory cell. The Input Gate consists of two components: the first is the Sigmoid function, which determines which information updates the memory cell; the second is the Tanh function, which generates new candidate memory information. These components are calculated as (3) and (4):

$$i_t = \sigma(W_i \cdot [h_{t-1}, x_t] + b_i) \quad (3)$$

$$\tilde{C}_t = tanh(W_C \cdot [h_{t-1}, x_t] + b_C) \quad (4)$$

Formula

f_t—— Output of the Oblivion Gate

h_{t-1}—— Hidden state from the previous moment

x_t—— Input features at the current time

W_t—— Weighting of the Oblivion Gate

b_f—— Bias of the Oblivion Gate

The Cell State is the core of LSTM, storing long-term memory. LSTM updates the memory cell state via the forget gate and input gate. The specific update formula is given by (5):

$$C_t = f_t \cdot C_{t-1} + i_t \cdot \tilde{C}_t \quad (5)$$

Formula

C_t—— The state of the memory cell at the current time

C_{t-1}—— The state of the memory cell from the previous moment

f_t—— The output of the forgetting gate controls how much of the previous memory should be forgotten

i_t—— The output of the input gate determines how the candidate memory information at the current time is added to the memory cell

The Output Gate determines the hidden state at the current time step, i.e., the output of the LSTM. The Output Gate is computed based on the current state of the memory cell, using the Sigmoid activation function to decide which information will be included in the final output. This is computed as (6) and (7):

$$o_t = \sigma(W_O \cdot [h_{t-1}, x_t] + b_o) \quad (6)$$

$$h_t = o_t \cdot \tanh(C_t) \quad (7)$$

Formula o_t The output gate controls which information is extracted from the memory cell

h_t The hidden state at the current time, which is the final output of the LSTM

To better understand the flow of the LSTM model, refer to **Fig. 2**.

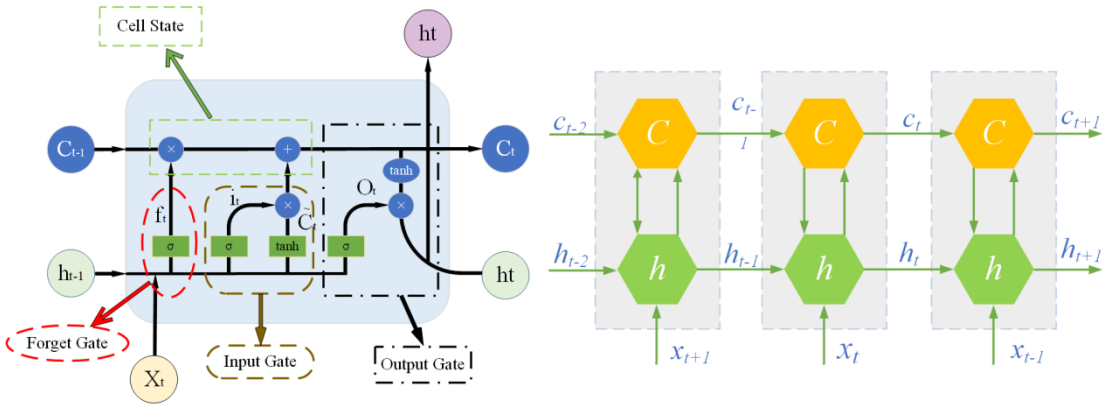

(a) LSTM grid structure diagram (b) LSTM extension diagram

Fig. 2 LSTM grid structure diagram and expansion diagram

As shown in **Fig. 2**, the network structure and flow diagram of the LSTM model illustrate how it handles information flow. The first step in the operation flow is to generate f_t by using h_{t-1} and x_t from the previous unit cell with the Sigmoid function (2), determining the information to retain in the memory cell before applying the forgetting gate. Next, h_{t-1} and x_t are used to generate it with the Sigmoid (3) and Tanh (4) functions, which determine the information to be added to the memory cell (input gate operation flow). Then, the new cell state $\tilde{C}_t$ is calculated using h_{t-1}, f_t, and i_t with (5), and the memory cell state is updated based on the outputs of the forget and input gates (cell state update process). Finally, O_t is generated using h_{t-1} and x_t with the Sigmoid function (6), and O_t and $\tilde{C}_t$ are used to generate the hidden state h_t at the current time step using the Tanh function (7) (output gate operation flow).

The following outlines the optimized design of the LSTM model to enhance its accuracy in rebar price prediction. **Figure 3** shows the basic flowchart of the optimized LSTM prediction model:

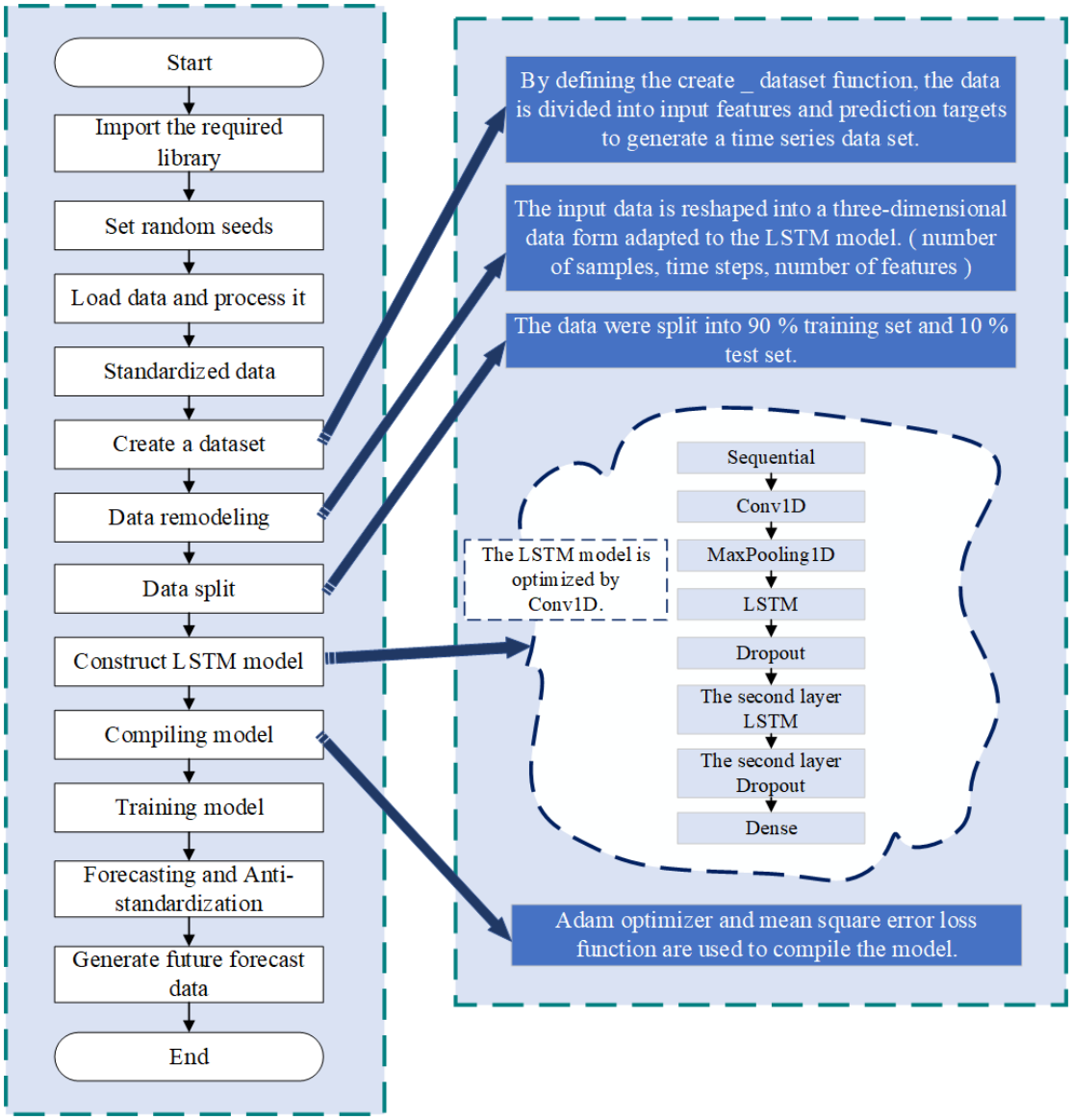

Figure 3 Flow chart of LSTM optimized prediction model

Figure 3 illustrates the basic flowchart of the optimized LSTM prediction model.

By adjusting the LSTM structure, optimizing hyperparameters, and incorporating external features, prediction accuracy can be further enhanced. LSTM can provide more accurate and stable predictions, especially when dealing with complex time series data. Furthermore, the LSTM model was optimized by incorporating a cascade structure that combines a Convolutional Neural Network (Conv1D) and LSTM. The number of LSTM layers was increased to improve the prediction accuracy of the model. Stacking multiple LSTM layers increases the model's expressive power, enabling it to capture more complex features. Interactions between multiple LSTM layers allow the model to learn deeper time series patterns. Hyperparameters, such as learning rate, batch size, and the number of nodes in the LSTM layer, are tuned to improve training speed and prediction accuracy. Dropout regularization is applied to prevent overfitting. Dropout is applied to prevent overfitting, particularly when data is limited, thus enhancing the model's generalization ability.

Additionally, the model incorporates relevant external features to further improve its predictions. As shown in **Fig. 2** and **Figure 3**, the design and optimization of the LSTM model provide a powerful tool for rebar price prediction, effectively capturing long-term dependencies and seasonal fluctuations in the data.

2.1.3 Modeling of BP Monomers

The BP neural network is a widely used feed-forward model that gradually adjusts the weights

and biases through the error backpropagation algorithm to minimize prediction error. This paper aims to construct a rebar price prediction model based on the BP neural network, analyze its nonlinear mapping ability to the price series, and optimize the network structure (e.g., hyperparameters such as the number of layers and nodes). The process of constructing the BP neural network is outlined in **Figure 4**.

Figure 4 illustrates how the BP neural network performs rebar price prediction, from the input layer to the output layer, through the nonlinear transformation of multiple layers of neurons and activation functions. The BP neural network learns patterns from historical data by adjusting weights and biases, enabling it to predict future prices based on these patterns. Additionally, relevant external features are incorporated to enhance prediction accuracy. While BP neural networks excel at nonlinear modeling, they face challenges such as long training times and sensitivity to noise. Combining other methods (e.g., LSTM, NeuralProphet) can help overcome these limitations and further enhance prediction accuracy.

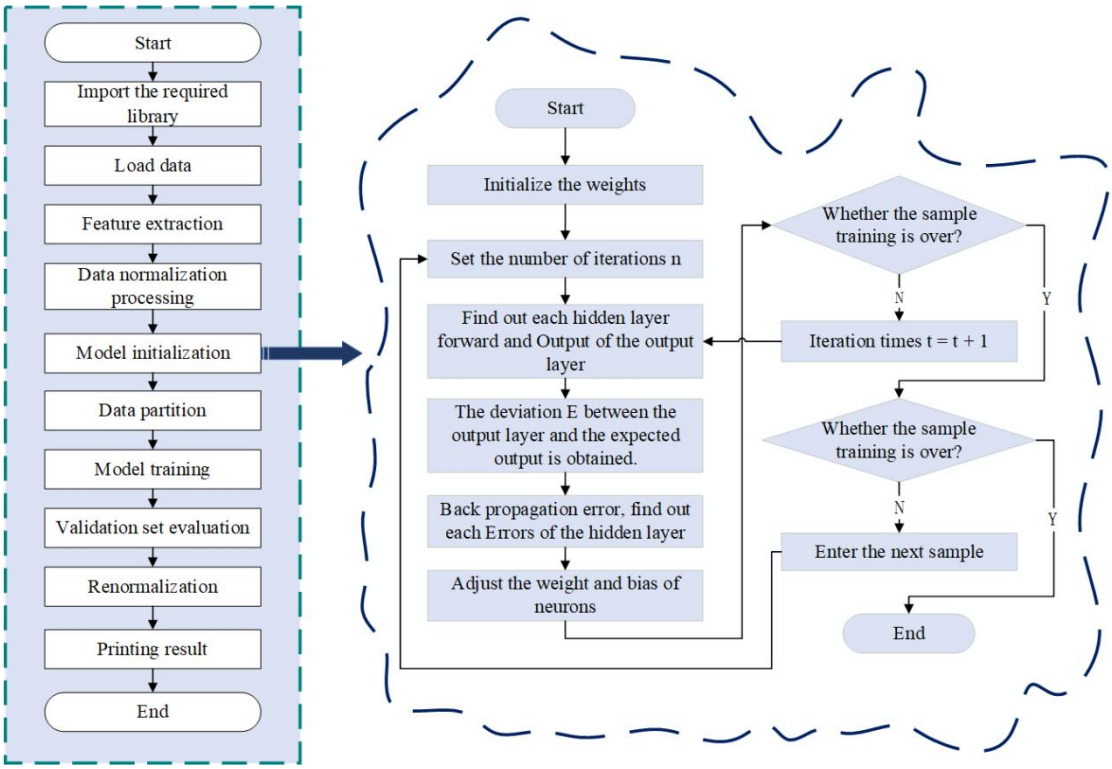

Figure 4 BP neural network model prediction process

2.2 Constructing a hybrid prediction model

To improve the prediction accuracy of single models, this study uses Stacking to combine different base prediction models into a hybrid model. Stacking is an ensemble learning method that enhances prediction accuracy by combining the outputs of different base learners (e.g., LSTM, NeuralProphet, BP neural network).

The core idea of Stacking is to train a meta-learner that uses the outputs of base learners as input to generate the final prediction. This approach allows Stacking to combine the strengths of multiple base models, reducing both bias and variance, and ultimately improving prediction performance. Specifically, Stacking captures more patterns by weightedly combining the outputs of multiple base learners, leading to more accurate predictions.

The following section will describe the construction process of the Stacking fusion model and demonstrate its flow with **Figure 5**.

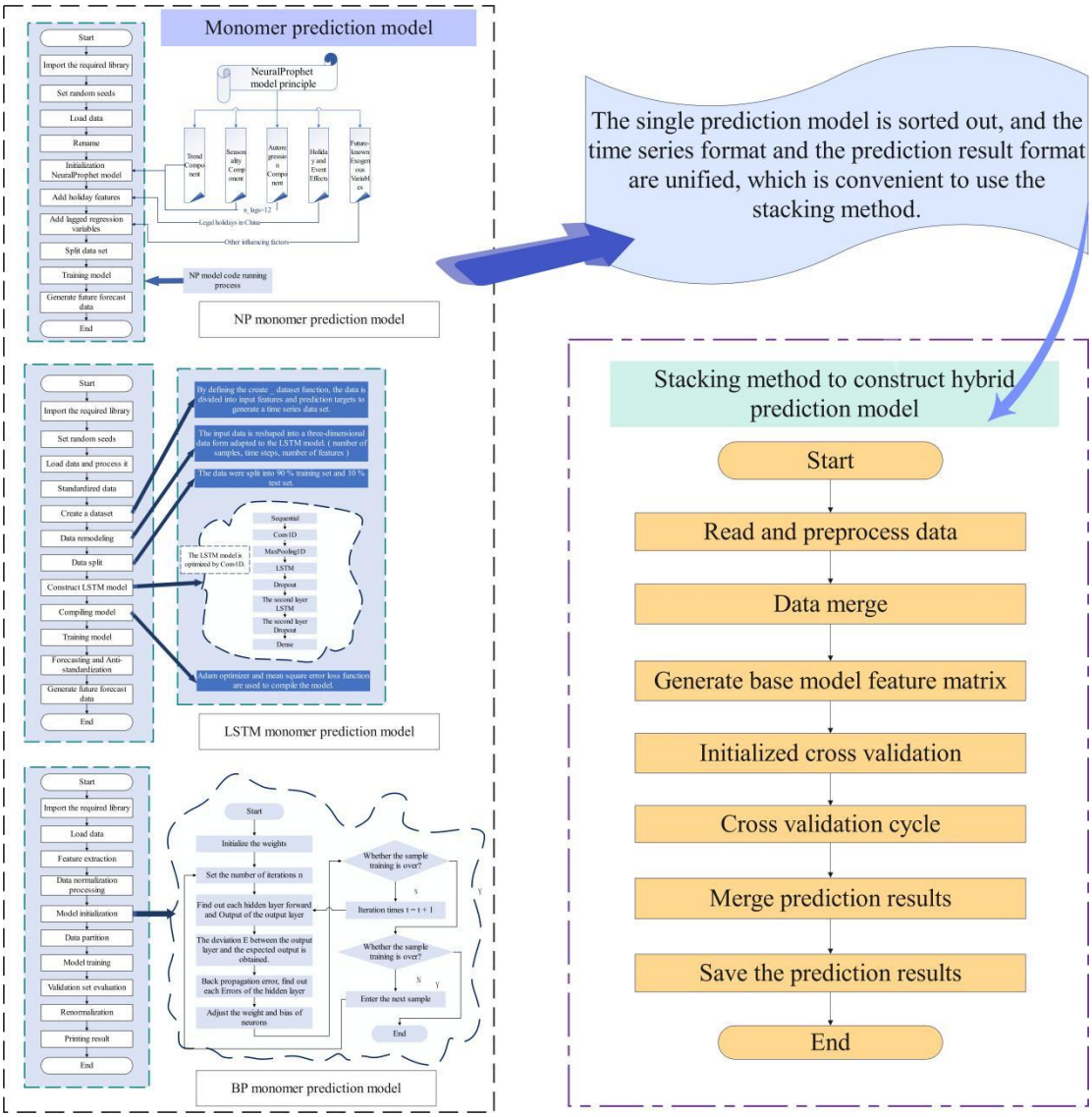

Figure 5 Stacking method to construct hybrid prediction model

As shown in **Figure 5**, the stacking method combines the predictions of models like LSTM, NeuralProphet, and BP neural network to predict the monthly price of Shijiazhuang rebar. The process involves three parts: first, the base learners (NP, LSTM, BP neural network) generate individual price predictions, which are passed to the next stage as input features. In the second part, the meta-learner trains by using the base learners' predictions as input features to a linear regression model (or other regression algorithm) for fusion. The meta-learner generates the final prediction by weighting the base learners' outputs. The meta-learner learns how to weight the base learners' outputs, improving the final prediction accuracy. This reduces bias and variance, improving the overall prediction accuracy. The third part involves analyzing and comparing the prediction results of the hybrid model with those of the individual models. The prediction errors (e.g., RMSE, MAE) of different models (LSTM, NeuralProphet, BP neural network, stacked model) are compared to verify whether stacking improves accuracy. A cross-sectional analysis evaluates the stacked models' performance in capturing price fluctuations, seasonality, and long-term trends, confirming whether stacking improves forecasting ability.

3 Experiments and Results

3.1 Data Collection and Pre-Processing

3.1.1 Data Collection

The accuracy of rebar price forecasts depends on the quality and completeness of the data used. The rebar price data used in this study are derived from the official information prices of Shijiazhuang City, Hebei Province. The information price refers to the official price

guidance for construction materials, periodically published by local government departments. It is widely used in project costing, budgeting, and market analysis, and is recognized for its authority and representativeness. In Shijiazhuang, the information price primarily reflects the comprehensive costs of construction materials, labor, equipment, and machinery within a specific period, serving as a reference for regional project pricing.

Rebar prices are influenced by various factors, including supply and demand dynamics, production costs, policies and regulations, the macroeconomic environment, and international market fluctuations. Thus, selecting authoritative and long-term continuous data is crucial. This study uses price data for φ16HRB400 Grade III rebar from January 2014 to September 2022, sourced from the Shijiazhuang Construction Engineering Cost Management Station and relevant government agencies. The data are expressed in CYN (Chinese Yuan) per ton, and the specific values are presented below (**Table 1**).

Rebar prices are influenced by various external factors, and their pricing mechanism is highly complex. In addition to direct factors such as market supply and demand, production costs, and policies, it also encompasses macroeconomic factors. Therefore, when constructing the prediction model, it is essential to integrate historical rebar price data with relevant influencing factors to enhance the model's accuracy.

This study collects data on factors influencing rebar prices from January 2014 to September 2022, covering dimensions such as raw material prices, energy factors, supply and demand, and macroeconomic conditions. All data are sourced from authoritative organizations to ensure their reliability and continuity. The specific influencing factors and data sources are presented in (**Table 2**).

Table 1 Price of φ16HRB400 Grade III rebar from January 2014 to September 2022 (unit: CNY /ton)

Mth / Year	Jan	Feb	Mar	Apr	May	Jun	Jul	Aug	Sep	Oct	Nov	Dec
2014	2650	2650	3600	3600	3600	3500	3500	3500	3500	3400	3200	3100
2015	2900	2900	2950	2950	2850	2700	2580	2680	2700	2600	2410	2250
2016	2350	2350	2450	3200	3050	2700	2800	2800	2850	2900	3000	3400
2017	3750	3750	4100	3800	3950	3900	4100	4350	4400	4350	4350	4700
2018	4200	4200	4350	4150	4310	4400	4500	4750	4950	4950	4400	4000
2019	4100	4100	4250	4400	4350	4350	4300	4100	4120	4050	4200	3950
2020	3850	3850	3800	3800	3800	4000	3950	3970	4070	4150	4100	4250
2021	4450	4450	5200	5650	5950	5450	5600	5550	5750	5650	5000	5000
2022	5000	5000	5200	5380	5380	4980	4400	4450	4350			

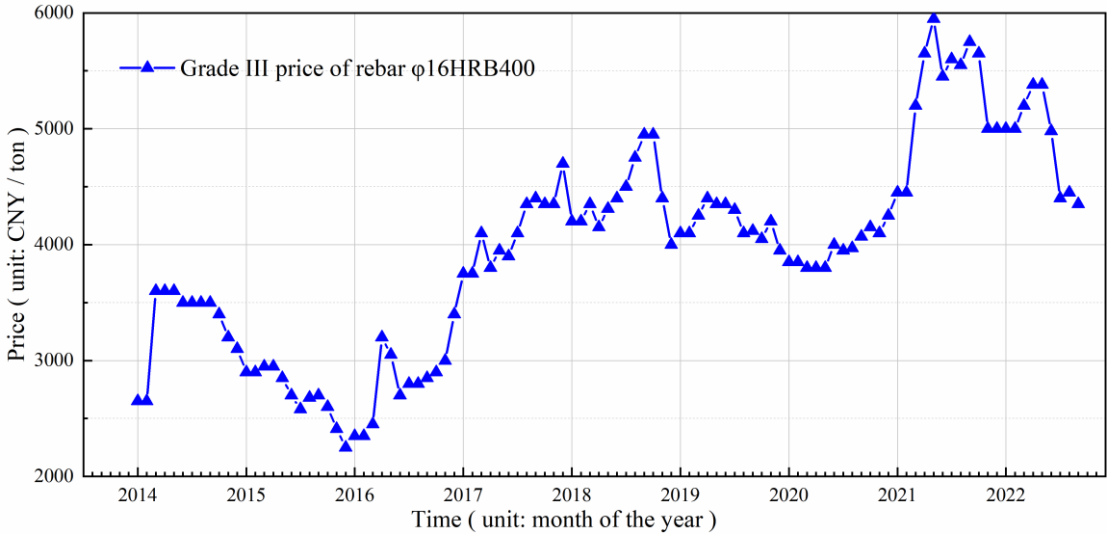

Figure 6 From January 2014 to September 2022, the price of φ16HRB400 grade III rebar (unit: CNY/ ton)

The selection of these influencing factors is based on a thorough analysis of rebar prices, encompassing the key factors driving price fluctuations. These factors will contribute to the development of a more comprehensive and accurate rebar price forecasting model.

Table 2 Influencing factors for rebar φ16HRB400 Grade III

Category	Name of influencing factor	Specific indictors	Data sources
Raw material price	Iron ore price	Absolute Iron Ore Price Indices (Tangshan, CYN / Wet Ton, Daily)	My steel mesh
	Coke prices	Absolute price of main coking coal (Tangshan, tax included, factory price, weekly)	My steel mesh
	Coal price	Coal Car Transportation Price (Xiaoyi→Shijiazhuang, CYN / ton, daily)	My steel mesh
	Scrap price	Heavy Waste Price (Shijiazhuang, ex-tax, Dalian market, CYN / ton, daily)	My steel mesh
Energy factors	Natural gas	Current value of natural gas production (ten thousand tons)	State statistical bureau
		Cumulative value of natural gas production (10,000 tons)	State statistical bureau
		Producer Price Indices of Natural Gas Extraction Industry (Same Month of Last Year = 100)	State statistical bureau
	Petroleum	Producer Price Indices (PPI) for Oil Extraction Industry (Same Month Last Year = 100)	State statistical bureau
	Electricity	Electricity production industry producer price index (the same month last year = 100)	State statistical bureau
Supply and	Iron and steel output	The current value of steel production (ten thousand tons)	State statistical bureau

demand		Cumulative value of steel production (ten thousand tons)	State statistical bureau
	Steel production	Reinforcement production current value (ten thousand tons)	State statistical bureau
		Cumulative value of steel reinforcement (ten thousand tons)	State statistical bureau
Macro factors	Investment in real estates	Cumulative value of real estate investment (billion CYN)	State statistical bureau

3.1.2 Data Pre-Processing

Data preprocessing is a crucial step in data analysis and modeling, aimed at enhancing data quality and providing a reliable foundation for subsequent analysis and prediction. Data cleaning, missing value imputation, outlier handling, and data storage for φ16HRB400 Grade III rebar price data and other influencing factors ensure the consistency and completeness of the time-series data, providing a reliable foundation for subsequent analysis and model development.

Data cleaning and preprocessing consists of four main steps. The first step is missing value imputation, where missing data for rebar prices or other influencing factors are addressed using interpolation or mean imputation methods to ensure data integrity. The second step is outlier detection and handling, where outliers in the data are identified using statistical methods and visualization tools (e.g., box plots, scatter plots) and are corrected or removed based on their characteristics. The third step is data standardization and normalization, which ensures equal contribution of different features during the training process. The data are standardized using the Z-score method and normalized using the Min-Max method. The final step is data storage, where the processed data are stored in a database or file to ensure consistency and reproducibility in subsequent analyses. These preprocessing steps ensure the consistency and completeness of the time series data, providing a reliable foundation for the construction of subsequent characterization and prediction models.

To identify the key factors influencing rebar price volatility, this study employs three methods: gray correlation analysis (GRA), multilayer perceptron (MLP), and Pearson correlation coefficient analysis. These methods assess the relationship between the characteristic and target variables from a multidimensional perspective and rank their importance.

Gray correlation analysis, based on gray system theory, evaluates the influence of variables on rebar prices by calculating the correlation coefficient between each characteristic and the target variable. The formula for calculating the correlation coefficient is presented in **Error! Reference source not found.**:

$$\xi_i(k)=\frac{\min_i \min_k \left|x_0(k)-x_i(k)\right|+\rho\cdot\max_i \max_k \left|x_0(k)-x_i(k)\right|}{\left|x_0(k)-x_i(k)\right|+\rho\cdot\max_i \max_k \left|x_0(k)-x_i(k)\right|} \quad (8)$$

.

Formula $x_0(k)$ —— Sequential values of the target variables

$x_i(k)$ —— Sequential values of the characteristic variables

ρ —— Resolution factor (typically 0.5)

To explore the nonlinear relationship between feature variables and the target variable, a multilayer perceptron (MLP) model was built using the Keras framework. The model consists of two hidden layers: the first with 64 neurons, the second with 32 neurons. The activation function is ReLU, and the output layer contains one neuron to generate the prediction. The model uses Mean Squared Error (MSE) as the loss function and Adam as the optimizer. During training, the data are normalized and split into training and test sets to ensure feature normalization and enhance the model's generalization ability. Training the multilayer feedforward neural network enables the model to automatically capture the complex nonlinear relationship between feature variables and rebar prices, offering valuable insights for feature selection.

Pearson's correlation coefficient measures the linear relationship between variables, calculated

as shown in (8):

$$\gamma = \frac{\sum (x_i - \bar{x})(y_i - \bar{y})}{\sqrt{\sum (x_i - \bar{x})^2 \cdot \sum (y_i - \bar{y})^2}} \quad (8)$$

In the formula, the value range of the Pearson correlation coefficient is [-1, 1]: +1 indicates a perfect positive correlation, 0 indicates no correlation, and -1 indicates a perfect negative correlation. The Pearson correlation coefficient effectively reflects the linear relationship between features and the target variable, aiding in identifying factors with a strong linear influence on rebar prices.

By integrating gray correlation analysis, MLP neural networks, and Pearson correlation coefficient analysis, this study identifies key variables significantly impacting rebar prices. The specific analysis results are presented in (**Table 3**).

As shown in **Table 2** and **Table 3**, the heavy waste price, the iron ore absolute price index, and the main coking coal absolute price are the most strongly correlated factors with rebar prices, with correlation coefficients of 0.816, 0.777, and 0.710, respectively. This indicates that fluctuations in raw material prices directly and significantly affect rebar prices. Gray correlation analysis reveals that the heavy waste price and iron ore price have the most significant influence on rebar prices. The importance scores from the multilayer feed-forward neural network indicate that natural gas production and iron ore prices exert a stronger influence on rebar prices. Especially in the complex market context, these variables can capture potential high-dimensional relationships. Pearson correlation coefficient analysis further confirms the influence of the heavy waste price, iron ore price, and the linear relationship between main coking coal prices and rebar prices.

Using the methodology described above, this study successfully identified key variables influencing rebar prices, including the iron ore price, main coking coal price, heavy scrap price, natural gas production, and the oil extraction industry price index.

Table 3 Results of correlation analysis between rebar prices and related characteristics

Specific indictors	Grey relational analysis	Multilayer feedforward neural network	Pearson correlation coefficient analysis
Absolute Iron Ore Price Indices (Tangshan, CYN / Wet Ton, Daily)	0.776716	9.207690	0.761088
Absolute price of main coking coal (Tangshan, tax included, factory price, weekly)	0.710347	8.449799	0.764871
Heavy Waste Price (Shijiazhuang, ex-tax, Dalian market, CYN / ton, daily)	0.816162	8.718645	0.890326
Current value of natural gas production (ten thousand tons)	0.717845	10.056078	0.633002
Cumulative value of natural gas production (10,000 tons)	0.672989	9.522925	0.276845
Producer Price Indices of Natural Gas Extraction Industry (Same Month of Last Year = 100)	0.641317	8.620737	0.307448
Producer Price Indices (PPI) for Oil Extraction Industry (Same Month Last Year = 100)	0.726405	8.943185	0.739185
Electricity production industry producer price index (the same month last year = 100)	0.721750	9.435205	0.519119
The current value of steel production (ten	0.724747	8.124369	0.490693

thousand tons)			
Cumulative value of steel production (ten thousand tons)	0.641667	8.993038	0.083961
Reinforcement production current value (ten thousand tons)	0.716127	8.369257	0.484818
Cumulative value of steel production (ten thousand tons)	0.646683	9.423933	0.113068
Cumulative value of real estate investment (billion CYN)	0.659886	6.611764	0.224740

This section supports the model's prediction by providing historical data through data collection and preprocessing. Several data analysis methods were employed to identify key factors that significantly impact rebar price fluctuations. The scientific rigor of the model construction and its prediction accuracy are ensured through feature importance assessment. These identified key variables will serve as important input features in the subsequent prediction model, further enhancing the accuracy of rebar price predictions.

3.2 Assessment Models

To comprehensively evaluate the performance of each predictive model, this study employed a range of common assessment metrics. The specific assessment metrics are outlined as follows:

MSE (Mean Squared Error) is a widely used metric to quantify the difference between predicted and actual values, calculated as shown in (9):

$$MSE = \frac{1}{n}\sum_{i=1}^{n}(y_i - \hat{y}_i)^2 \quad (9)$$

Where y_i is the actual value, $\hat{y}_i$ is the predicted value, and n is the sample size. A model with a lower MSE indicates that its predictions are closer to the actual values.

RMSE (Root Mean Squared Error) is the square root of MSE and is used to quantify the standard deviation between the predicted and actual values, providing a more intuitive measure of prediction error. The formula is as follows (10):

$$RMSE = \sqrt{\frac{1}{n}\sum_{i=1}^{n}(y_i - \hat{y}_i)^2} \quad (10)$$

A smaller RMSE indicates better model prediction accuracy.

RMLSE (Root Mean Squared Logarithmic Error) accounts for the logarithmic transformation of the data, which helps mitigate the impact of larger values on model evaluation. The formula is as follows (11):

$$RMLSE = \sqrt{\frac{1}{n}\sum_{i=1}^{n}(\log(y_i + 1) - \log(\hat{y}_i + 1))^2} \quad (11)$$

RMLSE effectively reduces the impact of extreme values on model evaluation, making it suitable for data with high volatility.

MAE (Mean Absolute Error) is the average of the absolute differences between predicted and actual values, offering a clear visualization of the model's prediction error. The formula is (12):

$$MAE = \frac{1}{n}\sum_{i=1}^{n}|y_i - \hat{y}_i| \quad (12)$$

A smaller MAE indicates more accurate model predictions.

MAPE (Mean Absolute Percentage Error) calculates the average relative error between actual and predicted values and is commonly used to compare model performance in predicting relative errors. Its formula is given by (13):

$$MAPE = \frac{1}{n}\sum_{i=1}^{n}\left|\frac{y_i - \hat{y}_i}{y_i}\right| \times 100\% \quad (13)$$

A smaller MAPE indicates a smaller relative error in the model's prediction and is commonly used to compare the prediction accuracy of different models.

The coefficient of determination (R^2) measures the goodness of fit of the regression model and indicates how well the independent variables explain the variation in the dependent variable. It is calculated as shown in (14):

$$R^2 = 1 - \frac{\sum_{i=1}^{n}(y_i - \hat{y}_i)^2}{\sum_{i=1}^{n}(y_i - \bar{y}_i)^2} \quad (14)$$

The value of R^2 ranges from 0 to 1, where values closer to 1 indicate that the model explains more of the variability.

The Theil's U statistic is used to compare the performance of a predictive model against a baseline model, such as stochastic or holdout predictions.It is calculated using the formula shown in (15):

$$U = \frac{\sqrt{\frac{1}{n}\sum_{i=1}^{n}(y_i - \hat{y}_i)^2}}{\sqrt{\frac{1}{n}\sum_{i=1}^{n}(y_i - y_{i-1})^2}} \quad (15)$$

The closer the Theil's U statistic is to 0, the better the predictive model's performance aligns with the ideal model.

By evaluating these indicators, the model's performance in terms of prediction accuracy, stability, and error tolerance can be assessed, providing a solid foundation for model optimization and selection.

3.3 Forecast Results and Analysis

Based on the historical data of rebar prices and influencing factors processed in Section 3.1, this paper predicts the rebar price from October 2022 to May 2024 using the constructed monolithic models: Neural Prophet (NP), LSTM, and BP neural network. The different monolithic prediction models are then fused into hybrid models using the stacking method. Three hybrid models—NP-LSTM, LSTM-BP, and NP-BP—are generated, and their prediction results are analyzed.

To assess the prediction accuracy of both single and hybrid models, this study uses several evaluation metrics: mean squared error (MSE), root mean squared error (RMSE), root mean squared logarithmic error (RMLSE), mean absolute error (MAE), mean absolute percentage error (MAPE), coefficient of determination (R^2), and Theil's U statistic. These evaluation metrics comprehensively assess the model's performance in terms of prediction accuracy, stability, and error tolerance, providing a solid foundation for model optimization and selection.

To verify the model's prediction accuracy, this paper compares the results of the single and hybrid models with the actual prices (Shijiazhuang City rebar price data from October 2022 to May 2024), as shown in **Figure 7**.

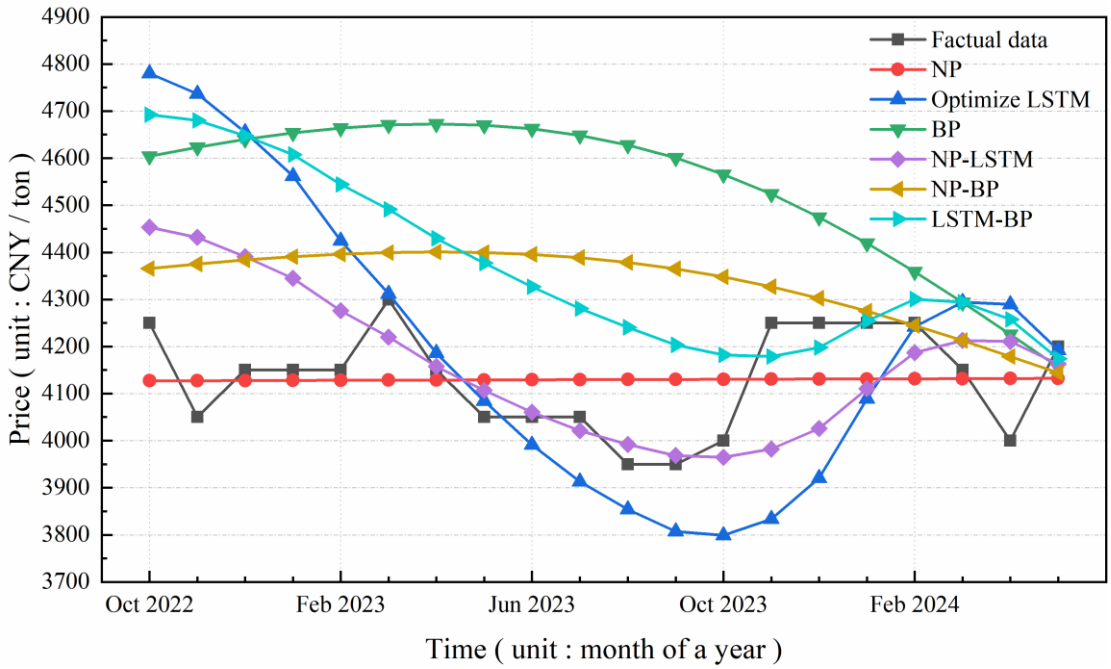

Figure 7 Comparison of predicted and actual prices (information price of φ16HRB400III rebar in Shijiazhuang from October 2022 to May 2024)

As shown in **Fig. 7**, the prediction results of the hybrid model are closer to the actual rebar price

data than those of the monolithic model. The monolithic model's predictions are more fluctuating, with a noticeable gap from the actual prices. In contrast, the hybrid model's predictions show higher consistency and are closer to the actual prices.It can be concluded that the hybrid forecasting model outperforms the monolithic model in accuracy.

Furthermore, based on the evaluation metrics provided in **Table 4**, the performance of each model can be analyzed in detail.

Table 4 Evaluation of prediction results

	MSE	RMSE	RMLSE	MAE	MAPE	R^2	Theil's U
NP	11599.706	107.701	0.011353	94.081	0.022850	-4599.948	68.657
Optimization LSTM	28832.755	169.802	0.018056	128.013	0.030666	-1.273	1.501
BP	1502450.960	1225.745	0.136326	1131.855	0.272969	-0.011853	1.006
NP-LSTM	25424.841	159.451	0.016469	121.626	0.029304	-0.057239	1.024
NP-BP	62365.169	249.730	0.025791	209.756	0.051573	-0.310106	1.166
LSTM-BP	91808.822	303.000	0.030529	252.960	0.061661	-0.052039	1.038

Based on **Figure 7** and **Table 4**, the following key conclusions can be drawn. For the monolithic models, the NP model shows the most accurate predictions, with the lowest prediction error according to the MSE, RMSE, and MAE metrics. In comparison, both the LSTM and BP models exhibit larger prediction errors, particularly the BP model, which has significantly higher errors than the others. Specifically, the NP model performed best across all assessment metrics, particularly in the MSE and RMSE. Analysis of R^2 and Theil's U statistics reveals that the BP model performs better in terms of stability, with a high coefficient of determination, indicating a better fit to the data. In contrast, the LSTM and NP models are less stable, with the NP model showing a negative coefficient of determination, indicating lower prediction stability.

For the hybrid prediction models, the NP-LSTM model performs better than the NP model in terms of R^2 and Theil's U, but shows lower MSE, RMSE, and MAPE compared to the LSTM and BP monolithic models. The NP-LSTM hybrid model performs well in terms of MSE, RMSE, and MAPE. Although the NP-LSTM model does not consistently outperform the single models, it combines the strengths of NeuralProphet and LSTM, effectively compensating for their shortcomings and improving overall prediction performance. Although the NP-BP and LSTM-BP hybrid models perform slightly worse than NP-LSTM, they still outperform the single models in certain evaluation metrics, further demonstrating that hybrid models are superior to single models. Hybrid models are generally more accurate and stable than single models. This demonstrates that hybrid models, by fusing different base learners through the stacking method, can provide more stable and accurate predictions.

By combining the strengths of different models through the stacking method, the hybrid model effectively addresses the limitations of monolithic models. LSTM and NeuralProphet excel in handling nonlinear relationships and long-term dependencies, while the stacking method enhances the prediction accuracy and stability of the model. Experimental results indicate that the stacked model better captures seasonal fluctuations and long-term trends in rebar prices, showing higher accuracy. Compared to the monolithic model, the hybrid model offers greater stability and generalization ability.

4 Conclusion

The hybrid model proposed in this paper, based on the stacking method, significantly enhances the prediction accuracy of rebar prices by combining LSTM and NeuralProphet. The stacking method effectively integrates the strengths of different models, enhancing overall prediction performance. Future research could optimize the model combinations in the stacking method further and investigate the contribution of other deep learning techniques (e.g., GRU) to time series forecasting. Based on the evaluation and analysis of the forecasting results, this paper presents the following conclusions:

1. This study identifies the key factors influencing the volatility of rebar prices. Specifically, the absolute iron ore price index,

the price of primary coking coal, the price of heavy scrap, the current value of natural gas production, and the ex-factory price index for industrial producers in the petroleum extraction sector were identified as key factors influencing rebar prices. These variables show high weights and significance in gray correlation analysis (GRA), multilayer feed-forward neural networks (MLP), and Pearson correlation coefficient analysis. They can explain linear changes in rebar prices and effectively capture nonlinear features, highlighting their central role in the rebar price formation mechanism.

2. The prediction results of the constructed monolithic model show that the NP model outperforms others in predicting rebar prices for 20 periods, with an RMLSE of 0.011353, MAPE of 0.022850, and Theil's U of 68.657.The LSTM optimization model has an RMLSE of 0.018056, MAPE of 0.030660, and Theil's U of 1.501.The BP model has an RMLSE of 0.136326, MAPE of 0.272969, and Theil's U of 1.006.Although the NP model has higher prediction accuracy, the LSTM optimization model performs better in terms of stability.
3. The Stacking method significantly enhances the prediction accuracy and stability of hybrid models by combining different base learner models. Compared to the monolithic model, it better integrates the strengths of each model, compensating for their weaknesses and providing more accurate predictions. This not only improves model performance, but also enhances its stability and reliability in real-world applications, adding significant value.
4. The NP-LSTM hybrid model, with an MSE of 25424.841, RMSE of 159.451, and MAPE of 0.029304, outperforms the LSTM-optimized monolithic model, which has an MSE of 28832.755, RMSE of 169.802, and MAPE of 0.030666. Moreover, its Theil's U of 1.024 is significantly better than the NP model's value of 68.657. These results demonstrate that the NP-LSTM model has a significant advantage in overall prediction capability.

The experimental results show that the hybrid prediction model, particularly NP-LSTM, offers significant advantages in predicting rebar prices, provides an effective predictive framework, and holds substantial practical value.

Author Contributions

All authors contributed to the study conception and design. Jingsi Hao: Writing–original draft, Visualization, Conceptualization, Data curation. Xiakai Wang: Methodology, Conceptualization, Writing–review & editing. Zhonghua Yang and Yuanyuan Zhao: Data curation, Supervision, Conceptualization. Kangjie Sun: Funding acquisition, Writing–review & editing.

Data Availability

All data used in this study are available publicly with sources provided in the Supplementary file.

Declarations

Ethical and Informed Consent for Data Used

This study used only publicly-available data. As such, ethical approval and informed con-sent for data usage were not required.

Conflict of Interest

The authors declare that they have no known competing financial interests or personal relationships that could have appeared to influence the work reported in this paper.

References

1. Wang F, Xue X, Hua J, et al. Properties of po lyoxymethylene fibre-reinforced seawater sea sand concrete exposed to high temperatures[J]. Construction and Building Materials, 2023, 409: 133854. https://doi.org/10.1016/j.conbui ldmat.2023.133854
2. Wang Q, Li L, Zhao Y, et al. Feasibility asses sment and application of sea sand in concrete production: A review[C]//Structures. Elsevier , 2024, 60. 105891. https://doi.org/10.1016/j.i struc.2024.105891
3. Feng X , Yang X ,Nie W , et al. Evaluating th e splitting capacity of timber beams loaded pe rpendicular to grain by bolted connections wit h steel plate. Experimental study and theoreti cal calculation[J]. Industrial Crops & Product s,2024,222(P3):119831-119831. https://doi.or g/10.1016/j.indcrop.2024.119831
4. Lyubomir L, Edmunds T, Nikolay A, et al. M odification of the roughness of 304 stainless s teel by laser surface texturing (LST)[J]. Laser Physics,2023,33 (4). https://doi.org/10.1088/1

555-6611/acbb76
5. Ryu W S, Choi P, Choi S, et al. Improvements of Full-Depth Repair Practices for Distresses in Continuously Reinforced Concrete Pavement[J]. Transportation Research Record,2013,2368(1):102-113. https://doi.org/10.3141/2368-10
6. Xu X, Zhang Y. Thermal coal price forecasting via the neural network[J]. Intelligent Systems with Applications, 2022, 14: 200084. https://doi.org/10.1016/j.iswa.2022.200084
7. Xuan Y, Yue Q. Forecast of steel demand and the availability of depreciated steel scrap in China[J]. Resources, Conservation and Recycling, 2016, 109: 1-12. https://doi.org/10.1016/j.resconrec.2016.02.003
8. Song L, Wang P, Hao M, et al. Mapping provincial steel stocks and flows in China: 1978-2050[J]. Journal of Cleaner Production, 2020, 262: 121393. https://doi.org/10.1016/j.jclepro.2020.121393
9. Liu Y, Li H, Guan J, et al. Influence of different factors on prices of upstream, middle and downstream products in China's whole steel industry chain. Based on Adaptive Neural Fuzzy Inference System[J]. Resources Policy, 2019, 60: 134-142. https://doi.org/10.1016/j.resourpol.2018.12.009
10. Kim K, Lim S. Price discovery and volatility spillover in spot and futures markets: evidences from steel-related commodities in China[J]. Applied Economics Letters, 2019, 26(5): 351-357. https://doi.org/10.1080/13504851.2018.1478385
11. Arık E, Mutlu E. Chinese steel market in the post-futures period[J]. Resources Policy, 2014, 42: 10-17. https://doi.org/10.1016/j.resourpol.2014.08.002
12. Xu X, Zhang Y. Network analysis of corn cash price comovements[J]. Machine Learning with Applications, 2021, 6: 100140. https://doi.org/10.1016/j.mlwa.2021.100140
13. He J, Wu J, Li H. Hedging house price risk in China[J]. Real Estate Economics, 2017, 45(1): 177-203. https://doi.org/10.1111/1540-6229.12147
14. Hu R, Zhang C. Discussion on energy conservation strategies for steel industry: based on a Chinese firm[J]. Journal of Cleaner Production, 2017, 166: 66-80. https://doi.org/10.1016/j.jclepro.2017.07.249
15. Wang J, Dong Y, Zhang K, et al. A numerical model based on prior distribution fuzzy inference and neural networks[J]. Renewable Energy, 2017, 112: 486-497. https://doi.org/10.1016/j.renene.2017.05.053
16. Wang P, Li W, Kara S. Cradle-to-cradle modeling of the future steel flow in China[J]. Resources, Conservation and Recycling, 2017, 117: 45-57. https://doi.org/10.1016/j.resconrec.2015.07.009
17. He K, Chen Y, Tso G K F. Price forecasting in the precious metal market: a multivariate EMD denoising approach[J]. Resources Policy, 2017, 54: 9-24. https://doi.org/10.1016/j.resourpol.2017.08.006
18. Wang C, Zhang S, Guo L. Investigation on the effective thermal conductivity of typical Pidgeon process briquette with a combined model[J]. International Journal of Heat and Mass Transfer, 2017, 115: 1348-1358. https://doi.org/10.1016/j.ijheatmasstransfer.2017.08.064
19. Yang J, Li Z, Wang T. Price discovery in Chinese agricultural futures markets: a comprehensive look[J]. Journal of Futures Markets, 2021, 41(4): 536-555. https://doi.org/10.1002/fut.22179
20. Xu X. Cointegration and price discovery in US corn cash and futures markets[J]. Empirical Economics, 2018, 55(4): 1889-1923. https://doi.org/
21. Xu X, Zhang Y. Individual time series and composite forecasting of the Chinese stock index[J]. Machine Learning with Applications, 2021, 5: 100035. https://doi.org/10.1016/j.mlwa.2021.100035
22. Xu X, Zhang Y. Dynamic relationships among composite property prices of major Chinese cities: contemporaneous causality through vector error corrections and directed acyclic graphs[J]. International Journal of Real Estate Studies, 2023, 17(1): 148-157. https://doi.org/10.11113/intrest.v17n1.294
23. Shayeghi H, Ghasemi A, Moradzadeh M, et al. Day-ahead electricity price forecasting using WPT, GMI and modified LSSVM-based S-OLABC algorithm[J]. Soft Computing, 2017, 21: 525-541. https://doi.org/10.1007/s00500-015-1807-1
24. Liu S, Jiang Y, Lin Z, et al. Data-driven two-step day-ahead electricity price forecasting considering price spikes[J]. Journal of Modern Power Systems and Clean Energy, 2022, 11(2): 523-533.https://doi.org/10.35833/MPCE.20

21.000196
25. Yuan C Z, San W W, Leong T W. Determining optimal lag time selection function with novel machine learning strategies for better agricultural commodity prices forecasting in Malaysia[C]//Proceedings of the 2020 2nd international conference on information technology and computer communications. 2020: 37-42. https://doi.org/10.1145/3417473.3417480
26. Wang D, Luo H, Grunder O, et al. Multi-step ahead electricity price forecasting using a hybrid model based on two-layer decomposition technique and BP neural network optimized by firefly algorithm[J]. Applied Energy, 2017, 190: 390-407. https://doi.org/10.1016/j.apenergy.2016.12.134
27. Zhou K, Yang S. Emission reduction of China′s steel industry: progress and challenges[J]. Renewable and Sustainable Energy Reviews, 2016, 61: 319-327. https://doi.org/10.1016/j.rser.2016.04.009
28. Supattana N. Steel price index forecasting using arima and arimax model[J]. National Institute of Development Administration, 2014.
29. Tcha M, Kim P J. Steel price projections. the economics of the East Asia steel industries[J]. 2019.
30. Chou M T, Huang B C. An analysis of the relationship between forward freight agreements and steel price index: An application of the vector ARMA model[J]. African Journal of Business Management, 2010, 4(6): 1149. https://doi.org/10.1177/1476750309349976
31. Zhao Y, Feng C, Xu N, et al. Early warning of exchange rate risk based on structural shocks in international oil prices using the LSTM neural network model[J]. Energy Economics, 2023, 126: 106921. https://doi.org/10.1016/j.eneco.2023.106921
32. Wang C, Xu G, Sun C, et al. Modeling and forecasting of coal price based on influencing factors and time series[J]. Journal of Cleaner Production, 2024, 467: 143030. https://doi.org/10.1016/j.jclepro.2024.143030
33. Liang Y, Lin Y, Lu Q. Forecasting gold price using a novel hybrid model with ICEEMDAN and LSTM-CNN-CBAM[J]. Expert Systems with Applications, 2022, 206: 117847. https://doi.org/10.1016/j.eswa.2022.117847
34. Jana R K, Ghosh I, Wallin M W. Taming energy and electronic waste generation in bitcoin mining: insights from Facebook prophet and deep neural network[J]. Technological Forecasting and Social Change, 2022, 178: 121584. https://doi.org/10.1016/j.techfore.2022.121584
35. Hu Y, Ni J, Wen L. A hybrid deep learning approach by integrating LSTM-ANN networks with GARCH model for copper price volatility prediction[J]. Physica A: Statistical Mechanics and its Applications, 2020, 557: 124907. https://doi.org/10.1016/j.physa.2020.124907
36. Usman U S, Salh Y H M, Yan B, et al. Fluoride contamination in African groundwater: Predictive modeling using stacking ensemble techniques[J]. Science of The Total Environment, 2024, 957: 177693. https://doi.org/10.1016/j.scitotenv.2024.177693
37. Balahang S, Ghodsian M. Enhancing rectangular side weir discharge prediction using stacking technique[J]. Flow Measurement and Instrumentation, 2024, 97: 102622. https://doi.org/10.1016/j.flowmeasinst.2024.102622
38. Hashim M, Khan L, Javaid N, et al. Stacked machine learning models for non-technical loss detection in smart grid: a comparative analysis[J]. Energy Reports, 2024, 12: 1235-1253. https://doi.org/10.1016/j.egyr.2024.06.015
39. Xu X, Zhang Y. Price forecasts of ten steel products using Gaussian process regressions[J]. Engineering Applications of Artificial Intelligence, 2023, 126: 106870. https://doi.org/10.1016/j.engappai.2023.106870
40. Cheng C H, Chen T L, Wei L Y. A hybrid model based on rough sets theory and genetic algorithms for stock price forecasting[J]. Information Sciences, 2010, 180(9): 1610-1629. https://doi.org/10.1016/j.ins.2010.01.014
41. Ghasemiyeh R, Moghdani R, Sana S S. A hybrid artificial neural network with metaheuristic algorithms for predicting stock price[J]. Cybernetics and systems, 2017, 48(4): 365-392. https://doi.org/10.1080/01969722.2017.1285162
42. Safari A, Davallou M. Oil price forecasting using a hybrid model[J]. Energy, 2018, 148: 49-58. https://doi.org/10.1016/j.energy.2018.01.007
43. Huang C F. A hybrid stock selection model using genetic algorithms and support vector regression[J]. Applied soft computing, 2012, 12(2): 807-818. https://doi.org/10.1016/j.asoc.2011.10.009